Reliable One-dimensional Approximate Solutions for Insulated Oblate Spheroid Containers

*King-Leung Wong, Shih-Shih Ku, Chung-Che Yang, Chun-Fa Wang, Yang-chin Chiu

***Abstract*—Since there is no reliable surface-area formula available for the calculation of the heat transfer characteristics of an insulated oblate spheroid, in this investigation, highly accurate oblate spheroid surface area is obtained by a simple numerical integration method. Based on the accurate oblate spheroid surface area, a reliable one-dimensional approximate solution of an insulated oblate spheroid container can be obtained with a one-dimensional RPSWT model. By comparing with accurate three-dimensional numerical results, it is found that in cases of low external convective coefficient (h_o =8.3 $Wm^{-2}K^{-1}$), long-short-axes ratio $a/b \leqq 3$, and insulation thickness $t/R_2 \leqq 2$, errors are within 3 %. In rarer situations with $a/b \leqq 5$ and $t/R_2 \leqq 2$, the errors are within 5.5 %. The above results are almost independent with the internal flow convective coefficient (h_i from 30 to 10^5 $Wm^{-2}K^{-1}$) and dimensionless container size ($0.5R_2ho/Ks$ from 1.55 to 155).**

***Index Terms*—insulation, oblate spheroid, *RPSWT* model, integral method**

I. Introduction

The insulation of hot and cold ducts and containers has been one of the most important engineering problems. Yet, simple constant surface area plate thermal resistance (***PTR***) model has long been the main stream method to analyze the heat transfer characteristics of insulated polygonal ducts or polyhedron containers. This model assumes that the insulated surface area of the external insulation is the same as that of a bare duct or container, a practice neglecting the excessive surface area caused by insulation layer thickness, which in turn significantly reduces the magnitude of heat transfer rate. Wong et al. [1] proposed a plane wedge thermal resistance (***PWTR***) model aimed to investigate the heat-transfer characteristics associated with insulated polygonal pipes. In general, if the one-dimensional ***PWTR*** model is used to analyze the two-dimensional heat transfer problems of insulated polygonal ducts, accuracy deteriorates with decreasing the number of edges. Therefore, Wong et al. [2] studied the heat-transfer characteristics of an insulated long rectangular or square duct ***64-CPWTR*** model. Wong et al. [3] extended the various ***CPWTR*** models to obtain a reliable one-dimensional model for insulated regular polygonal ducts.

As far as an insulated container is concerned, Wong and Chou [4] developed a regular polygonal-top solid wedge thermal-resistance (RPSWT) model to obtain the heat transfer characteristics of an insulated regular polyhedron; Chen et al. [5] used combined 60% and RPSWT model and 40% PTR model to obtain a reliable one-dimensional method applied to heat-transfer problems associated with insulated rectangular tanks. Recently, Chen et al. [6] proposed a reliable model for an insulted oval duct using one-dimensional PWTR model and 91-CPWTR model based on very accurate oval perimeter obtained by a simple numerical integration method. In the present investigation, a follow-up study to Chen et al. [6], the results are calculated by one-dimensional RPSWT model [4] based on highly accurate oblate spheroid surface areas calculated by a reliable simple numerical integration method extended from Chen et al. [6]. The results are compared with those of three-dimensional numerical results for insulated oblate spheroid containers with different long-short-axes ratios, from 1.5 to 5, and with three group dimensionless container sizes and in several practical thermal conditions.

Manuscript received October 7, 2008. This work was supported in part by the National Science Council of Taiwan under Grant NSC-97-2221-E168-044-MY2.

*King-Leung Wong is with the Kun-Shan University of Technology, 949, Da-Wan Road, Yung-Kang City, Tainan County, Taiwan 710; (corresponding author, phone: +886-62057121; fax:+886-62050509 e-mail::klwong@mail.ksu.edu.tw).

Shih-Shih Ku is with the National Taipei University of Technology, No.1, Sec.3, Chung-Hsiao E. Rd., Taipei City, Taiwan 106 (e-mail: kuss@tnvtc.gov.tw).

Chung-Che Yang is with the National Tainan Qi-Zhi School, No.74, Sec.2,Chang-Her Rd., An-Nan District, Tainan City, Taiwan 709 (e-mail: jasonycc2007@pchome.com.tw).

Chun-Fa Wang is with the Air-Water Technology Co.,Ltd, No.12, Lane.115, Cai-Kong 1St. Rd., Tzuo-Ying District, Kaohsiung City, Taiwan 813 (e-mail: wang@airwater.com.tw).

Yang-chin Chiu is with the Kun-Shan University of Technology, 949, Da-Wan Road, Yung-Kang City, Tainan County, Taiwan 710 (e-mail: k1234kh@yahoo.com.tw)

II. Problem Formulation

Fig. 1 shows the bare oval cross-sectional profile at x-y coordinates of an insulated oblate spheroid container with the external half-long-axis length of a, half-short-axis length of b, wall thickness of t_1, wall conductivity of K_1. An insulation layer with thickness of t and conductivity of K_s is wrapped around the oblate spheroid. The oblate spheroid is then assumed to be exposed to internal and external fluids with convection heat transfer coefficients of h_i and h_o and temperatures of T_i and T_o, respectively. In addition, Fig. 2 shows that various oblate spheroid containers with different long-short-axes ratios a/b of 1.5, 2, 3, 4 and 5, transformed from a bare sphere with the same external surface area, are analyzed in this study.

A. The oblate spheroid container's surface area

The following approximate oval perimeter formula [7] has been conventionally used to analyze the characteristics of oval duct:

$$L = 2\pi\sqrt{\frac{a^2+b^2}{2}} \tag{1}$$

The equation of the oval cross-sectional profile of an oblate spheroid container shown in Fig. 3 is:

$$\frac{x^2}{a^2}+\frac{y^2}{b^2}=1 \quad (2)$$

The perimeter of the oval cross-sectional profile can then be divided into $\boldsymbol{n}$ line segments. As shown in Fig. 3, the two end points for the i^{th} line segment can be expressed as:

$$x_i = a\cos(2i\pi/n) \quad (3)$$

$$y_i = b\sin(2i\pi/n) \quad (4)$$

$$x_{i+1} = a\cos[2(i+1)\pi/n] \quad (5)$$

$$y_{i+1} = b\sin[2(i+1)\pi/n] \quad (6)$$

From the definition of the line segment, the perimeter of the oval profile [18] can be obtained by the following summation:

$$L_{E2}=\sum_{\theta=0}^{2\pi}\sqrt{(x_{i+1}-x_i)^2+(y_{i+1}-y_i)^2} \quad (7)$$

Due to the axial symmetry of the geometry of an oblate spheroid, the external surface area of a bare oblate spheroid container can be obtained by the following summation:

$$A_{E2}=\sum_{\theta=0}^{\pi}2\pi y_i\sqrt{(x_{i+1}-x_i)^2+(y_{i+1}-y_i)^2} \quad (8)$$

Similarly, accurate internal oblate spheroid surface area, $\boldsymbol{A_{E1}}$, can be obtained by replacing the values of $\boldsymbol{a}$ and $\boldsymbol{b}$ by $\boldsymbol{(a-t_1)}$ and $\boldsymbol{(b-t_1)}$, respectively in equations (3) to (6) and (8); meanwhile, accurate external insulation surface area, $\boldsymbol{A_{E3}}$, can be obtained by replacing the values of $\boldsymbol{a}$ and $\boldsymbol{b}$ by $\boldsymbol{(a+t)}$ and $\boldsymbol{(b+t)}$ in equations (3) to (6) and (8), respectively.

The approximated perimeter and surface area would be highly accurate if the number $\boldsymbol{n}$ is very large. If $\boldsymbol{a}=\boldsymbol{b}=1$, equation (2) becomes a circle. In the case of $\boldsymbol{n}=10^6$, the error generated from equation (7), compared with the exact perimeter of the circle, is about 10^{-5}; and the error generated from equation (8), compared with the exact surface area of a sphere ($\boldsymbol{a}=\boldsymbol{b}=1$), is about 10^{-6}. For the sake of obtaining reliable results, $n=10^6$ is also adopted in the present investigation to obtain the oblate spheroid surface area. Even with this huge number of segmentations, it only takes only about an insignificant 2 second CPU time in a PC to complete the numerical integration. Due to the extreme small errors generated by equations (7) and (8), the approximate values can be regarded as the exact perimeter and surface area.

Since there is no appropriate surface area formula for an oblate spheroid container, the approximate oval perimeter from equation (1) can be extended, to obtain an approximate oblate spheroid surface area as:

$$S=2\pi(a^2+b^2) \quad (9)$$

By compared with the exact value, the error of oval perimeter generated by equation (1) can be expressed as:

$$E_L=\frac{L-L_{E2}}{L_{E2}}\times 100\% \quad (10)$$

Similarly, the error of oblate spheroid surface area generated by equation (9) can be expressed as:

$$E_S=\frac{S-A_{E2}}{A_{E2}}\times 100\% \quad (11)$$

The errors of equations (10) and (11) are shown in Fig. 4. It can be seen that the greater the long-short-axes ratio $\boldsymbol{a/b}$ is, the larger the values of $\boldsymbol{E_L}$ and $\boldsymbol{E_S}$ are. Between them, $\boldsymbol{E_S}$ is much larger than $\boldsymbol{E_L}$. From Fig. 4, it is obvious that any calculation based on equation (9) is inaccurate; therefore, the oblate spheroid surface area shouldn't be obtained by equation (9).

B. The equivalent sphere based on accurate oblate spheroid surface area

The heat transfer characteristics of an insulated oblate spheroid can be calculated by using the concept of equivalent sphere based on the same bare external surface area. The outer radius $\boldsymbol{R_2}$ of the equivalent bare sphere is:

$$R_2=\left(\frac{A_{E2}}{4\pi}\right)^{1/2} \quad (12)$$

$\boldsymbol{R_2}$ is also used for dimensionless thickness, $\boldsymbol{t/R_2}$. Since the critical radius of an insulated sphere is $2\boldsymbol{K_s}/\boldsymbol{h_0}$ [15], the dimensionless insulated oblate spheroid container size can be expressed as $0.5\boldsymbol{R_2 h_0/K_s}$.

The internal and external surface-areas of equivalent bare sphere are:

$$A_{C1}=4\pi(R_2-t_1)^2 \quad (13)$$

$$A_{C2}=4\pi(R_2)^2=A_{E2} \quad (14)$$

and the external surface area of the equivalent insulated sphere is:

$$A_{C3}=4\pi(R_2+t)^2 \quad (15)$$

III. The Heat Transfer Rate with One-Dimensional RPSWT Mode

The thermal resistance of one-dimensional RPSWT model is:

$$R_{th}=\frac{t}{K_s\sqrt{A_2A_3}} \quad (16)$$

From Fig. 2, if $\boldsymbol{a}=\boldsymbol{b}$, an insulated oblate spheroid becomes an insulated sphere. Then the relations of t, A_2, and A_3 of an insulated sphere can be written as:

$$t=R_3-R_2,\ A_2=4\pi R_2^2, \text{ and } A_3=4\pi R_3^2 \quad (17)$$

Therefore, the thermal resistance of a sphere can also be obtained by substituting equation (17) into equation (16) as follows:

$$R_{th}=\left[\frac{t}{K_s\sqrt{A_2A_3}}\right]=\frac{1}{4\pi K_s}\left(\frac{1}{R_2}-\frac{1}{R_3}\right) \quad (18)$$

It can be seen from equation (18) that the thermal resistance of an insulated sphere is a special case of the RPSWT model because a sphere can be approached by increasing the number of faces of a polyhedron to infinity.

A. Heat transfer rate based on accurate surface area and with RPSWT model

The heat transfer rate of an insulated oblate spheroid container with RPSWT model and based on accurate surface area is:

$$Q_W = \frac{(T_i - T_o)}{\frac{1}{h_i A_{E1}} + \frac{t_1}{K\sqrt{A_{E1}A_{E2}}} + \frac{t}{K_S\sqrt{A_{E2}A_{E3}}} + \frac{1}{h_o A_{E3}}} \quad (19)$$

And its error compared with three-dimensional numerical heat transfer rate, Q_n, is:

$$E_W = (\frac{Q_E - Q_n}{Q_n}) \times 100\,\% \quad (20)$$

B. Heat transfer rate of an equivalent insulated sphere based on accurate oblate spheroid surface area

The heat transfer rate of an equivalent insulated sphere based on accurate oblate spheroid surface area is:

$$Q_C = \frac{(T_i - T_o)}{\frac{1}{h_i A_{C1}} + \frac{1}{4\pi K}(\frac{1}{R_1} - \frac{1}{R_2}) + \frac{1}{4\pi K_S}(\frac{1}{R_2} - \frac{1}{R_3}) + \frac{1}{h_o A_{C3}}} \quad (21)$$

And its error compared with three-dimensional numerical heat transfer rate, Q_n, is:

$$E_C = (\frac{Q_C - Q_n}{Q_n}) \times 100\,\% \quad (22)$$

IV. Energy Equation and Boundary Conditions

The heat conduction governing equation for a three-dimensional insulated oblate spheroid is:

$$\frac{\partial}{\partial x}(K\frac{\partial T}{\partial x}) + \frac{\partial}{\partial y}(K\frac{\partial T}{\partial y}) + \frac{\partial}{\partial z}(K\frac{\partial T}{\partial z}) = 0 \quad (23)$$

The boundary conditions are:

$$h_i(T_i - T_s)_{A_1} = -K(\frac{\partial T}{\partial N})_{A_1} \quad (24)$$

$$-K_s(\frac{\partial T}{\partial N})_{A_3} = h_o(T_s - T_o)_{A_3} \quad (25)$$

$$(\frac{\partial T}{\partial N})_{symmetrical.boundary} = 0 \quad (26)$$

where N is the normal direction on any surface, and T_s represents the surface temperature of the insulation layer.

V. Numerical Two-Dimensional Heat Transfer Results

Equations (23) to (26) are solved by an in-house USTREAM code developed by the third named author to obtain the three-dimensional numerical heat transfer results. In order to check if the numerical results are reliable, an insulated sphere is analyzed to determine how many cells are needed to obtain a satisfactory result. It was found that a model of an insulated sphere, which consists of 26600 cells, gave a satisfactory solution of heat transfer rate within ±0.01% compared with that from exact analytic solution. Therefore, in the case of analyzing an insulated oblate spheroid, the numerical solutions obtained by the model with same number of cells can be expected to be highly accurate.

VI. Results and Discussions

The results of the oblate spheroid container with various long-short-axes ratios a/b of 1.5, 2, 3, 4 and 5 in practical situations of external convection heat transfer coefficients h_o=8.3 $Wm^{-2}K^{-1}$, wall conductivity K_1=77 $Wm^{-1}K^{-1}$, insulation layer conductivity K_S=0.035 $Wm^{-1}K^{-1}$, internal fluid temperature T_i=100℃ and external fluid temperature T_o=0℃ with various dimensionless container size ($0.5R_2h_o/K_s$) and internal heat convection coefficient h_i are shown in Figs. 5~7 and Tables 1~3, respectively. The relations of heat transfer rate error, E_W, calculated by one-dimensional ***RPSWT*** model with accurate surface area, and heat transfer rate error, E_C, of an insulted equivalent sphere based on accurate external surface area of a bare oblate spheroid versus dimensionless insulated thickness, t/R_2, in situation of dimensionless container size, $0.5R_2h_o/K_S$=1.55~2.75, with h_i=10^5 $Wm^{-2}K^{-1}$ are shown in Fig. 5 and Table 1, which lists the detail data. The relations of E_W and E_C vs. t/R_2 in cases of $0.5R_2h_o/K_S$=15.5~27.5 with h_i=30 $Wm^{-2}K^{-1}$ are shown in Fig. 6 and Tables 2. The relations of E_W and E_C vs. t/R_2 in cases of $0.5R_2h_o/K_S$=94.8~155.0 with h_i=10^5 $Wm^{-2}K^{-1}$ are shown in Fig. 7 and Table 3.

It is found from Figs.5~7 and Tables 1~3 that in situations of $a/b \leqq 3$ and $t/R_2 \leqq 2$, $E_W \leqq 3$ %; and in other rarer situations with $a/b \leqq 5$ and $t/R_2 \leqq 2$, $E_W \leqq 5.5$ %, the results are almost independent with the convective coefficient of internal fluid h_i and dimensionless container size if a model is based on accurate external surface area of a bare oblate spheroid. However, the heat transfer rate errors, E_C are almost twice as large as those of E_W.

VII. Conclusion

This study shows that approximate surface area formula is not suitable to be applied to an insulated oblate spheroid to obtain reliable heat-transfer results. In order to achieve a higher level of accuracy, an integration method, which returns very accurate surface area, introduced in this study needs to be used. Since using equivalent sphere based on the same external surface area of a bare oblate spheroid generates higher errors, reliable one-dimensional ***RPSWT*** model based on accurate surface area should be employed to calculate the heat transfer characteristic of an insulated oblate spheroid container. This only requires a PC incorporated with a small computer code in any language (such as LabVIEW in this study) without the need to use CFD software. As demonstrated in this study, reliable heat-transfer results can easily be obtained by this simple practice. It is very suitable to engineering application.

References

[1] KL Wong , HM Chou and YH Li, Complete Heat Transfer Solutions of an Insulated Regular Polygonal duct by Using a PWTR Model, Energy Conversion and Management, 45, (2004), p.1705~1724.

[2] KL Wong, TL Hsien, P Richards and BS Her, The reliable simple one-dimensional 64-CPWTR model applied to the two-dimensional heat transfer problem of an insulated rectangular duct in an air conditioning or refrigeration system, International Journal of Refrigeration, 28, (2005), p.1029-1039.

[3] KL Wong, A Al-Jumaily and TH Lu, Reliable one-dimensional CPWTR models for two-dimensional insulated polygonal ducts, International Journal of Refrigeration, 30, (2007), p. 254-266.

[4] KL Wong and HM Chou, Heat Transfer Characteristics of an Insulated Regular Polyhedron by Using a Regular Polygonal Top Solid Wedge Thermal Resistance Model, Energy Conversion and Management, 44, (2003), p.3015~3036.
[5] WL Chen , KL Wong and HM Chou, A reliable one-dimensional method applied to heat-transfer problems associated with insulated rectangular tanks in refrigeration systems, International Journal of Refrigeration 29, (2006) p. 285-294.
[6] WL Chen, KL Wong, TL Hsien and CT Huang, Reliable one-dimensional approximate solution of an insulated oval duct, Energy Management & Conversion, 48, (2007) p.3135-3145.
[7] HB William, CRC standard mathematical table, 25th edition, Chemical Rubber Pub., Cleveland, (1978), p.14

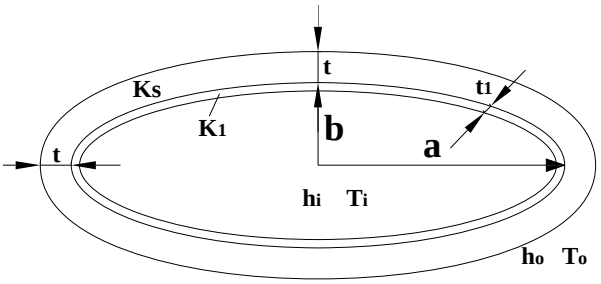

Fig.1 The parameters of an insulated oblate spheroid container

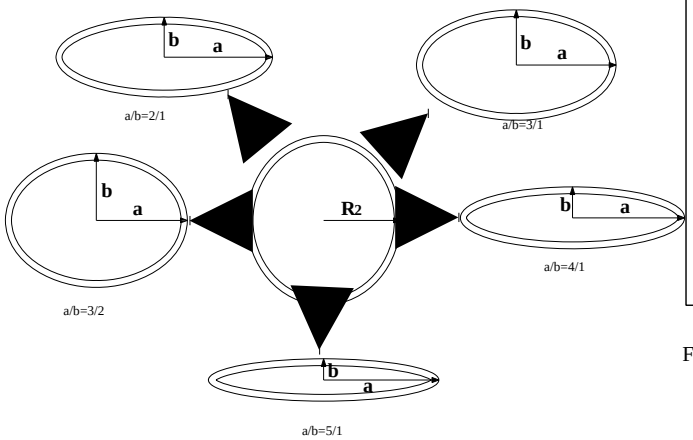

Fig. 2 The oblate spheroid with various long-short-axes ratios *a/b*, transformed from a bare sphere with the same external surface area

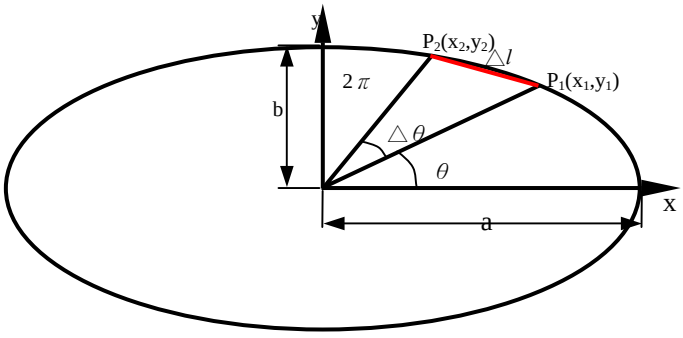

Fig. 3 The oval cross-sectional profile of an oblate spheroid and its relative parameters

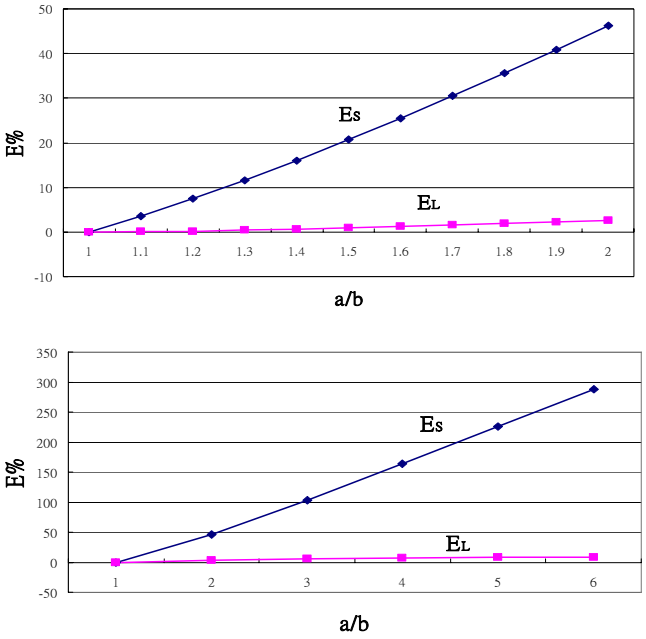

Fig. 4 The errors generated by approximate formulas of oval perimeter and oblate spheroid surface area versus long-short-axes ratio *a/b*

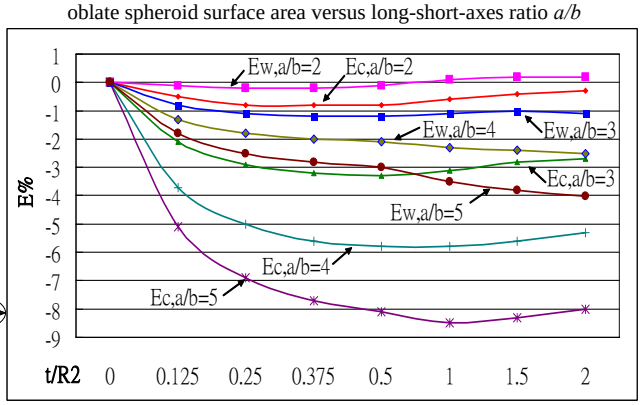

Fig.5 The relations of E_W and E_C vs. t/R_2 as well as various a/b in situation of dimensionless size $0.5R_2h_o/K_S$=1.55~2.75 with h_i=10^5 $Wm^{-2}K^{-1}$, t_1=1mm, K_1=77 $Wm^{-1}K^{-1}$, K_S=0.035 $Wm^{-1}K^{-1}$, h_o=8.3 $Wm^{-2}K^{-1}$, T_i=100℃ and T_o=0℃

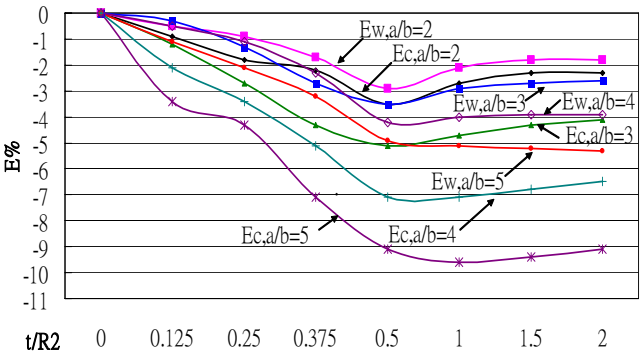

Fig.6 The relations of E_W and E_C vs. t/R_2 as well as various a/b in situation of dimensionless size $0.5R_2h_o/K_S$=15.5~27.5 with h_i=30 $Wm^{-2}K^{-1}$, t_1=2mm, K_1=77 $Wm^{-1}K^{-1}$, K_S=0.035 $Wm^{-1}K^{-1}$, h_o=8.3 $Wm^{-2}K^{-1}$, T_i=100℃ and T_o=0℃

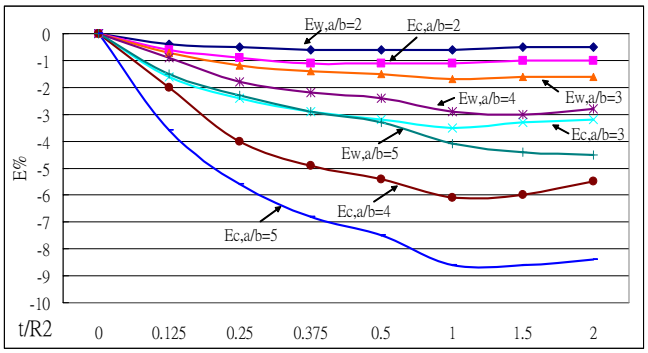

Fig.7 The relations of E_W and E_C vs. t/R_2 as well as various a/b in situation of dimensionless size $0.5R_2h_o/K_S$=94.8~155.0 with h_i=10^5 $Wm^{-2}K^{-1}$, t_1=5mm, K_1=77 $Wm^{-1}K^{-1}$, K_S=0.035 $Wm^{-1}K^{-1}$, h_o=8,3 $Wm^{-2}K^{-1}$, T_i=100℃ and T_o=0℃

Table

Table 1. In situation of h_i=10^5 $Wm^{-2}K^{-1}$ with t_1=1 mm, K_1=77 $Wm^{-1}K^{-1}$, K_S=0.035 $Wm^{-1}K^{-1}$, h_o=8.3 $Wm^{-2}K^{-1}$, T_i=100℃ and T_o=0℃, the relations of E_W and E_C vs. t/R_2 as well as various a/b

(a) a/b=1.5; a=0.03m, b=0.02 m; R_2=0.0232 m, $0.5R_2h_O/K_S$=2.75

t/R_2	t,mm	Q_W,Wm^{-1}	Q_C,Wm^{-1}	Q_n,Wm^{-1}	E_W,%	E_C,%
0	0	5.616	5.616	5.609	0.0	0.0
0.25	5.802	3.231	3.227	3.228	0.1	0.0
0.5	11.60	2.469	2.465	2.464	0.2	0.0
1.0	23.21	1.874	1.871	1.869	0.2	0.1
1.5	34.81	1.625	1.622	1.620	0.3	0.1
2.0	46.41	1.488	1.486	1.4835	0.3	0.2

(b) a/b=2; a=0.02 m, b=0.01 m; R_2=0.01307 m, $0.5R_2h_O/K_S$=1.55

t/R_2	t, mm	Q_W, Wm^{-1}	Q_C, Wm^{-1}	Q_n, Wm^{-1}	E_W, %	E_C, %
0.0	0	1.782	1.782	1.778	0.0	0.0
0.25	3.268	1.423	1.415	1.426	-0.2	-0.8
0.5	6.537	1.215	1.206	1.216	-0.1	-0.8
1.0	13.07	0.997	0.990	0.996	0.1	-0.6
1.5	19.61	0.888	0.882	0.886	0.2	-0.4
2.0	26.15	0.823	0.819	0.821	0.2	-0.3

(c) a/b=3; a=0.03 m, b=0.01 m; R_2=0.01567 m; $0.5R_2h_O/K_S$=1.858

t/R_2	t,mm	Q_W,Wm^{-1}	Q_C,Wm^{-1}	Q_n,Wm^{-1}	E_W,%	E_C,%
0.0	0	2.564	2.564	2.558	0.0	0.0
0.25	3.920	1.888	1.853	1.909	-1.1	-2.9
0.5	7.840	1.556	1.523	1.574	-1.2	-3.3
1.0	15.68	1.241	1.216	1.254	-1.1	-3.1
1.5	23.52	1.092	1.072	1.104	-1	-2.8
2.0	31.36	1.006	0.990	1.017	-1.1	-2.7

(d) a/b=4; a=0.04 m, b=0.01 m; R_2=0.0179 m; $0.5R_2h_O/K_S$=2.128

t/R_2	t,mm	Q_W, Wm^{-1}	Q_C, Wm^{-1}	Q_n, Wm^{-1}	E_W, %	E_C, %
0	0	3.361	3.361	3.353	0	0
0.25	4.488	2.329	2.254	2.373	-1.8	-5
0.5	8.976	1.874	1.804	1.914	-2.1	-5.8
1.0	17.95	1.466	1.413	1.500	-2.3	-5.8
1.5	26.93	1.280	1.238	1.312	-2.4	-5.6
2.0	35.90	1.174	1.140	1.204	-2.5	-5.3

(e) a/b=5; a=0.05 m, b=0.01 m; R_2=0.01998 m; $0.5R_2h_O/K_S$=2.368

t/R_2	t mm	Q_W, Wm^{-1}	Q_C, Wm^{-1}	Q_n, Wm^{-1}	E_W, %	E_C, %
0	0	4.165	4.166	4.156	0.2	0.2
0.25	4.996	2.749	2.623	2.819	-2.5	-6.9
0.5	9.993	2.173	2.058	2.234	-3	-8.1
1.0	19.99	1.676	1.590	1.737	-3.5	-8.5
1.5	29.98	1.454	1.387	1.512	-3.8	-8.3
2.0	39.97	1.329	1.274	1.385	-4	-8

Table 2. In situation of h_i=30 $Wm^{-2}K^{-1}$ with t_1=1 mm, K_1=77 $Wm^{-1}K^{-1}$, K_S=0.035 $Wm^{-1}K^{-1}$, h_o=8.3 $Wm^{-2}K^{-1}$, T_i=100℃ and T_o=0℃, the relations of E_W and E_C vs. t/R_2 as well as various a/b

(a) a/b=1.5; a=0.3m, b=0.2 m; R_2=0.232 m, $0.5R_2h_O/K_S$= 27.5

t/R_2	t,mm	Q_W,Wm^{-1}	Q_C,Wm^{-1}	Q_n,Wm^{-1}	E_W,%	E_C,%
0	0	439.1	439.1	439.1	0.0	0.0
0.25	58.02	47.15	47.10	48.33	-0.3	-0.6
0.5	116.0	29.50	29.46	29.98	-1.6	-1.7
1.0	232.1	20.06	20.03	20.28	-1.1	-1.3
1.5	348.1	16.81	16.79	16.97	-0.9	-1.1
2.0	464.1	15.17	15.15	15.30	-0.8	-1.0

(b) a/b=2; a=0.2 m, b=0.1 m; R_2=0.1307 m, $0.5R_2h_O/K_S$=15.5

t/R_2	t,mm	Q_{Wt},Wm^{-1}	Q_{Ct},Wm^{-1}	Q_n,Wm^{-1}	E_W,%	E_C,%
0	0	139.1	139.2	139.2	0.0	0.0
0.25	32.68	25.14	25.03	26.25	-0.9	-1.8
0.5	65.37	16.21	16.12	16.69	-2.9	-3.5
1.0	130.7	11.18	11.12	11.42	-2.1	-2.7
1.5	196.1	9.411	9.362	9.582	-1.8	-2.3
2.0	261.5	8.506	8.465	8.645	-1.8	-2.3

ISBN: 978-988-17012-7-5

(c) a/b=3; a=0.3 m, b=0.1 m; R_2=0.1568 m; $0.5R_2h_O/K_S$=18.6

t/R_2	t,mm	Q_W,Wm^{-1}	Q_C,Wm^{-1}	Q_n,Wm^{-1}	E_W,%	E_C,%
0	0	200.2	200.3	200.3	0.0	0.0
0.25	39.20	31.09	30.68	32.51	-1.3	-2.7
0.5	78.40	19.89	19.55	20.60	-3.5	-5.1
1.0	156.8	13.66	13.41	14.07	-2.9	-4.7
1.5	235.2	11.47	11.27	11.78	-2.7	-4.3
2.0	313.6	10.34	10.18	10.61	-2.6	-4.1

(d) a/b=4; a=0.4 m, b=0.1 m; R_2=0.1795 m; $0.5R_2h_O/K_S$=21.3

t/R_2	t,mm	Q_W,Wm^{-1}	Q_C,Wm^{-1}	Q_n,Wm^{-1}	E_W,%	E_C,%
0	0	262.5	262.6	262.5	0	0
0.25	44.88	36.49	35.63	38.26	-1.1	-3.4
0.5	89.76	23.25	22.54	24.26	-4.2	-7.1
1.0	179.5	15.93	15.41	16.59	-4	-7.1
1.5	269.3	13.34	12.94	13.89	-3.9	-6.8
2.0	359.0	12.02	11.68	12.50	-3.9	-6.5

(e) a/b=5; ; a=0.5 m, b=0.1 m; R_2=0.1998 m; $0.5R_2h_O/K_S$= 23.7

t/R_2	t,mm	Q_W,Wm^{-1}	Q_C,Wm^{-1}	Q_n,Wm^{-1}	E_W,%	E_C,%
0	0	325.4	325.6	325.4	0.0	0.0
0.25	49.96	41.47	40.06	43.63	-2.1	-4.3
0.5	99.93	26.38	25.22	27.73	-4.9	-9.1
1.0	199.8	18.04	17.20	19.01	-5.1	-9.6
1.5	299.8	15.09	14.43	15.92	-5.2	-9.4
2.0	399.7	13.57	13.02	14.33	-5.3	-9.1

Table 3. The detail relations of E_W and E_C vs. t/R_2 as well as various a/b in situation of dimensionless size $0.5R_2h_o/K_S$=94.8~155.0 with h_i=10^5 $Wm^{-2}K^{-1}$, t_1=5mm, K_1=77 $Wm^{-1}K^{-1}$, K_S=0.035 $Wm^{-1}K^{-1}$, h_o=8.3 $Wm^{-2}K^{-1}$, T_i=100℃and T_o=0℃

(a) a/b=1.5; a=1.5m, b=1m; R_2=1.16m, $0.5R_2h_O/K_S$= 137.6

t/R_2	t,m	Q_W,Wm^{-1}	Q_C,Wm^{-1}	Q_n,Wm^{-1}	E_W,%	E_C,%
0	0	14039	14039	14038	0.0	0.0
0.25	0.290	252.49	252.23	253.08	-0.2	-0.3
0.5	0.580	152.56	152.36	152.97	-0.3	-0.4
1.0	1.160	102.04	101.88	102.27	-0.2	-0.4
1.5	1.740	85.095	84.972	85.276	-0.2	-0.4
2.0	2.320	76.604	76.503	76.762	-0.2	-0.3

(b) a/b=2; a=2 m, b=1 m; R_2=1.307 m, $0.5R_2h_O/K_S$ =155.0

t/R_2	t,m	Q_W,Wm^{-1}	Q_C,Wm^{-1}	Q_n,Wm^{-1}	E_W,%	E_C,%
0.0	0	17825	17825	17822	0.0	0.0
0.25	0.326	285.70	284.57	287.17	-0.5	-0.9
0.5	0.653	172.68	171.76	173.74	-0.6	-1.1
1.0	1.307	115.48	114.82	116.14	-0.6	-1.1
1.5	1.961	96.268	95.752	96.746	-0.5	-1.0
2.0	2.614	86.627	86.205	87.048	-0.5	-1.0

(c) a/b=3; a=2.1 m, b=0.7 m; R_2=1.097 m; $0.5R_2h_O/K_S$= 130.2

t/R_2	t,m	Q_W,Wm^{-1}	Q_C,Wm^{-1}	Q_n,Wm^{-1}	E_W,%	E_C,%
0.0	0	12563	12563	12560	0	0
0.25	0.274	241.53	238.43	244.36	-1.2	-2.4
0.5	0.548	146.58	144.08	148.83	-1.5	-3.2
1.0	1.097	98.158	96.361	99.804	-1.7	-3.5
1.5	1.646	81.77	80.373	83.127	-1.6	-3.3
2.0	2.194	73.505	72.363	74.717	-1.6	-3.2

(d) a/b=4; a=2 m, b=0.5 m; R_2=0.898 m; $0.5R_2h_O/K_S$=106.4

t/R_2	tm	Q_W,Wm^{-1}	Q_C,Wm^{-1}	Q_n,Wm^{-1}	E_W,%	E_C,%
0	0	8402.2	8402.3	8400.5	0.0	0.0
0.25	0.224	199.06	194.47	202.66	-1.8	-4.0
0.5	0.448	121.41	117.70	124.43	-2.4	-5.4
1.0	0.897	81.439	78.771	83.850	-2.9	-6.1
1.5	1.346.	67.790	65.715	69.887	-3.0	-6.0
2.0	1.796	60.867	59.171	62.643	-2.8	-5.5

(e) a/b=5; a=2 m, b=0.4 m; R_2=0.799 m; $0.5R_2h_O/K_S$= 94.8

t/R_2	tm	Q_W,Wm^{-1}	Q_C,Wm^{-1}	Q_n,Wm^{-1}	E_W,%	E_C,%
0	0	6664.7	6664.8	6663.3	0.0	0.0
0.25	0.199	178.87	172.88	183.12	-2.3	-5.6
0.5	0.399	109.57	104.74	113.28	-3.3	-7.5
1.0	0.799	73.611	70.135	76.730	-4.1	-8.6
1.5	1.199	61.226	58.518	64.025	-4.4	-8.6
2.0	1.598	54.908	52.694	57.524	-4.5	-8.4